Available online at www.sciencedirect.com

ScienceDirect

Procedia Engineering 2 (2010) 743–750

Procedia Engineering

www.elsevier.com/locate/procedia

Fatigue 2010

High Cycle Fatigue Behaviour of Magnesium Alloys

L.Nascimento*, S.Yi, J.Bohlen, L. Fuskova, D. Letzig, K.U. Kainer

MagIC – Magnesium Innovation Centre, GKSS Research Centre Geesthacht GmbH, Geesthacht D21502, Germany

Received 26 February 2010; revised 10 March 2010; accepted 15 March 2010

Abstract

The influence of crystallographic texture on fatigue failure mechanisms was studied by comparing the fatigue behaviour of two extruded magnesium alloys, AZ31 and ZN11. The microstructures and fracture surfaces of specimens were examined using scanning electron microscopy (SEM) to reveal the micromechanisms of fatigue crack initiation. The AZ31 alloy has an inhomogeneous grain structure and strong fibre texture, which cause strong asymmetry in the tensile and compressive yield strengths. This yield stress asymmetry is related to the high twinning activity under compressive loading. The metallographic investigation reveals that the cracks are mainly initiated at twin boundaries. On the other hand, a weak texture and fully recrystallised, homogeneous grain structure are found in the experimental alloy ZN11 after extrusion. As a consequence, twinning is suppressed and no yield stress asymmetry is observed. The fatigue failure of ZN11 is initiated by cyclic slip deformation.

Keywords: Wrought magnesium alloy, high cycle fatigue, crystallographic texture, crack initiation

1. Introduction

Magnesium alloys are attractive for structural applications since they offer suitable properties such as light weight, high specific strength and good castability. In recent years the application of wrought magnesium alloys has been increasing due to the fact that they have superior mechanical properties compared to cast alloys [1]. Wrought magnesium alloys have great potential for use as engineering components in the automotive industry and in some aerospace applications [2]. Since a considerable number of these engineering components are used under dynamic loading conditions, knowledge on the fatigue behaviour of wrought magnesium alloys is required. Although extensive work has been done on the mechanical properties of wrought magnesium alloys, detailed information on the fatigue behaviour, especially in the high cycle regime, is still lacking [3]. With regard to high cycle fatigue, it has been suggested that crack initiation may take up most of the fatigue life [4]. Thus, in order to optimise the fatigue behaviour of Mg-alloys, determination of the crack initiation mechanisms is necessary. Published work has suggested that fatigue failure can be induced by three different mechanisms: (i) cyclic deformation, (ii) an environmental influence on cyclic slip or (iii) deformation caused by mechanical twinning. The cyclic deformation mechanism is associated with the irreversible deformation that builds up during the fatigue test through the interaction between slip bands and grain boundaries. This leads to local stress concentrations and then to crack

* Corresponding author. Tel.: +49-0452-87-1911; fax: +49-04152-87-1927.
E-mail address: ligia.nacimento@gkss.de

1877-7058
doi:10.1016/j.proeng.2010.03.080

initiation, which usually occurs at the surface [5, 6]. The second mechanism suggested, the environmental influence on cyclic slip [7], involves the combination of an aggressive environment, in this case air, with cyclic slip. The formation of an oxide layer on the surface or near to the surface during the fatigue test is thought to hinder cyclic slip and the local stress concentrations generated finally lead to crack initiation. Deformation caused by twinning has also been pointed out as a possible crack initiation factor [8], especially when wrought magnesium alloys are considered, since these alloys are generally characterised by strong crystallographic textures and tensile/compression yield stress asymmetries.

In this study, fatigue tests were performed on wrought magnesium alloys with different textures in order to determine the influence of the crystallographic texture on crack initiation mechanisms. Extrusion experiments were carried out using two magnesium alloys, one is the conventional wrought magnesium alloy AZ31, and the other is an experimental alloy ZN11 which contains neodymium. As it is well established that the addition of rare earth elements leads to the formation of textures [9, 10] distinctly different from conventional AZ31, using an alloy such as ZN11 allows investigation of the influence of the different initial textures on the mechanical behaviour. The mechanical properties were determined by means of tensile, compression and rotating bending tests. The microstructures and fracture surfaces of specimens were examined using optical microscopy and scanning electron microscopy (SEM) in order to investigate the micro-mechanisms of fatigue crack initiation.

2. Experimental

2.1. Materials and extrusion conditions

The chemical compositions of the alloys used in this study are given in Table 1. Cast billets were homogenised at 350 °C and 400 °C, respectively, for 15 hours. Round profiles with a diameter of 350 mm were machined from the homogenised billets and were indirectly extruded at 350 °C with an extrusion ratio of 1:30. Ram speeds of 2.8 mm/s for AZ31 and 1.0 mm/s for ZN11 were used in order to produce similar average grain sizes.

Table 1. Chemical composition of the materials investigated (wt.%)

Alloy	Al	Nd	Zn	Mg
AZ31	2.72	0	0.90	Balance
ZN11	0	0.81	0.92	Balance

2.2. Texture measurements and microstructural analysis

In order to analyse the microstructure by optical microscopy, standard metallographic sample preparation techniques were employed, including the use of an etchant based upon picric acid [11], which revealed the microstructural details. Optical microscopy and SEM analysis were used to investigate the microstructures and crack front-profiles. The crystallographic texture was measured using an X-ray diffractometer (Panalytical) with CuK_{α} radiation in the reflection geometry. The (00.2), (10.0), (10.1), (10.2) and (11.0) pole figures were measured and the inverse pole figures in the extrusion direction were calculated.

2.3. Mechanical Tests

The specimens used for tensile as well as compression testing were machined in the extrusion direction. Tensile specimens with a gauge length of 30 mm and a diameter of 6 mm were used. Tensile and compression tests were carried out using a universal testing machine (Zwick Z050) at room temperature with an initial strain rate of 10^{-3} s^{-1}. Fatigue specimens with a diameter of 8 mm and a gauge length of 60 mm were machined in the extrusion direction. Prior to fatigue testing, the surfaces of the specimens were mechanically polished with 0.3 μm diamond paste.

Fatigue tests were carried out using a rotating bending fatigue testing machine (Zwick UBM 200) operating at a frequency of 70 Hz at room temperature in air.

3. Results and discussion

3.1. As-extruded state

The microstructure of AZ31 in the as-extruded condition is illustrated in Fig. 1a. This alloy shows an inhomogeneous grain structure consisting of both large and small equiaxed grains. In addition, some unrecrystallised grains elongated in the extrusion direction (ED) are observed. In contrast to AZ31, a very homogeneous microstructure is observed in ZN11, Fig. 1b. The average grain sizes of AZ31 and ZN11 are about 11 µm and 9 µm, respectively.

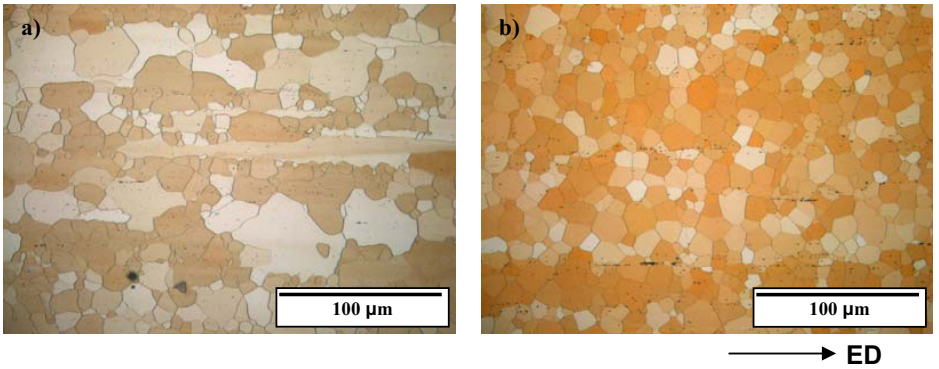

Fig. 1. Microstructures of as-extruded alloys (a) AZ31 and (b) ZN11

The AZ31 alloy (Fig 2a) exhibits a strong texture with high intensities distributed along the planes (10.0) and (11.0). In contrast, the ZN11 alloy shows a texture distinct from that found in the classical wrought Mg alloys after round extrusion. The texture of this experimental alloy is characterised by its very weak intensity. Moreover, the maximum intensity in the inverse pole figure is found at the pole corresponding to the c-axes being tilted about 60° from the extrusion direction. Recently published studies have shown that the weak textures found in alloys containing rare earth elements are strongly related to a retardation of recrystallisation and grain growth [9, 10, 12]. The fine, homogeneous microstructure observed in the present ZN11 alloy is in agreement with this argument. In contrast, the microstructure of the AZ31 alloy shows evidence of grain growth. Moreover, the strong intensity at the <10.0> pole in the AZ31 alloy confirms the presence of unrecrystallised grains, as reported in [13].

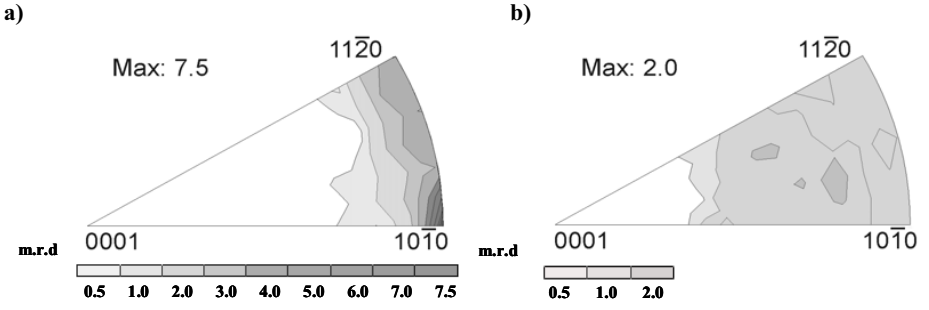

Fig. 2. Inverse pole figures parallel to the extrusion direction of a) AZ31 and b) ZN11 in the as-extruded condition

SEM imaging of the microstructure of ZN11 revealed stringers of particles oriented in the extrusion direction. The particles were found in the α-Mg matrix as well as at grain boundaries (Fig. 3). SEM-EDX analysis indicated very high contents of neodymium and zinc in the particles.

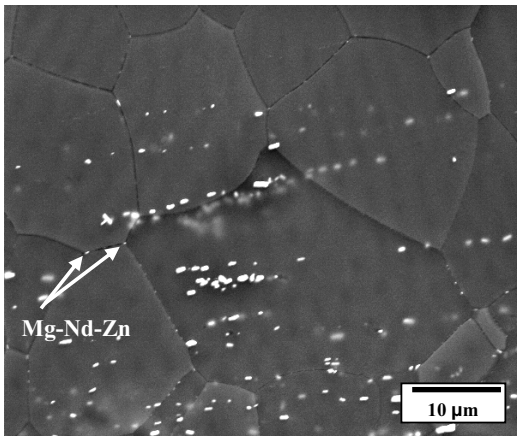

Fig. 3. SEM image (SE) of the ZN11 alloy, intermetallic (Mg-Nd-Zn) particles at the grain boundaries.

This intermetallic phase, Mg-Nd-Zn, appears to be broken up and dispersed along the extrusion direction. The homogeneous microstructure of ZN11 suggests that recrystallisation, in this case, dynamic recrystallisation (DRX), occurred during extrusion. Wenjiang et al. [14] have reported that the Mg-Nd-Zn particles restrict the growth of dynamically recrystallised grains during processing. The presence of the particles at the grain boundaries, together with a solute drag effect involving the heavy element Nd, could be responsible for the impeded grain growth and the weak texture of the ZN11 alloy, Fig. 2.

3.2. Mechanical Characterisation

The results of the tensile and compression tests are shown in Table 2. The alloy AZ31 exhibits a significant mechanical yield asymmetry. As reported extensively in the literature, the crystallographic texture has a strong influence on the mechanical properties [15, 16]. This effect is also observed in the mechanical properties of AZ31 and ZN11. These alloys exhibit completely different initial textures and consequently different mechanical properties. This is a result of the fact that at room temperature plastic deformation in magnesium alloys occurs mainly by dislocation glide and twinning [15].

Table 2. Mechanical properties of the alloys

Alloy	Tensile Yield Strength (TYS) (MPa)	Ultimate Tensile strength (UTS)(MPa)	Elongation (%)	Compressive Yield Strength (CYS) (MPa)	Ultimate Compressive strength (UCS)(MPa)	Elongation (%)
ZN11	108	210	39	100	323	16
AZ31	197	269	19	109	352	10

Under tensile loading, the AZ31 alloy exhibits a high yield stress and relatively low work hardening up to the maximum stress. However, under compressive loading a low yield stress and high subsequent work hardening are observed. This mechanical asymmetry is related to the fibre texture in AZ31 and the fact that several

unrecrystallised grains remained after extrusion. Under tensile loading, the preferred orientation of the basal planes does not favour the operation of tensile twinning or basal slip and the result is a high tensile yield stress and low work hardening. Under compressive loading the preferred orientation of the basal planes leads to extensive {10-12} twinning. Further deformation is hindered when a high density of tensile twins is present in the microstructure, since twin boundaries can act as obstacles to dislocation glide [17]. Consequently, strong work hardening is achieved. Furthermore, larger and unrecrystallised grains tend to show high densities of tensile twins, which corresponds well to earlier findings on the influence of grain size on the activation of twinning [18]. For the ZN11 alloy, the tensile yield strength and compressive yield strength are very similar. This can also be explained by the crystallographic texture and microstructure. Since this alloy has a very weak texture with the basal planes tilted with respect to the extrusion direction, plastic deformation by dislocation slip is favoured and {10-12} twinning is less attractive. Moreover, differences in the activation of {10-12} twins in compression and tension are not expected and consequently, no mechanical asymmetry is observed. In addition, the ZN11 alloy exhibits a fully recrystallised, homogeneous microstructure, which also hinders deformation twinning.

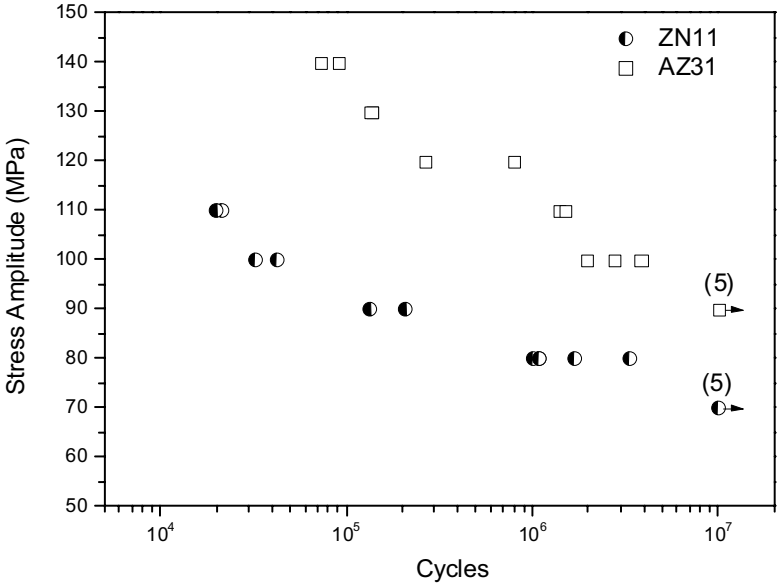

Fig. 4. S-N curves for AZ31 and ZN11; the arrows indicate runout conditions and the numbers the quantity of runout samples, respectively.

The S-N diagrams for AZ31 and ZN11 are shown in Fig. 4. The endurance limit of AZ31 at 10^7 cycles is 90 MPa. The fatigue ratio calculated using the compressive yield strength is equivalent to 0.82. On the other hand, when the fatigue ratio (fatigue strength/TYS or CYS) is calculated using the tensile yield strength the fatigue ratio is 0.45. This difference can be explained by the yield asymmetry, as pointed out previously. The yield asymmetry plays a key role in rotating bending tests, since the sample undergoes half cycles under tension and half cycles under compression. It is worthwhile to point out again that the compressive yield strength is significantly lower than the tensile yield strength in the AZ31 alloy, which is explained by the favourable orientation for {10-12} twinning under compression along the ED. Consequently, at stress amplitudes lower than the TYS but above the CYS, the sample experiences plastic deformation via twinning in the compressive half cycle, while no plastic deformation occurs in the tensile half cycle. The endurance limit of ZN11 at 10^7 cycles is 70 MPa and the fatigue ratio is 0.7. In this case the value of the fatigue ratio calculated using the TYS or the CYS is almost the same, since this alloy does not exhibit the yield asymmetry.

The fracture surfaces of each sample configuration are exhibited in Fig. 5. It can be observed that for both alloys fatigue failure originates mainly at the surface of the specimens, as is generally observed in fatigue specimens fractured by rotating bending. On the fracture surface of the AZ31 sample (Fig. 5a), some quasi-cleavage regions can be seen. On the other hand, some quasi-cleavage regions, Mg-Nd-Zn particles and the oxide layer are observed on the fracture surface of ZN11 alloy, as indicated in Fig. 5b.

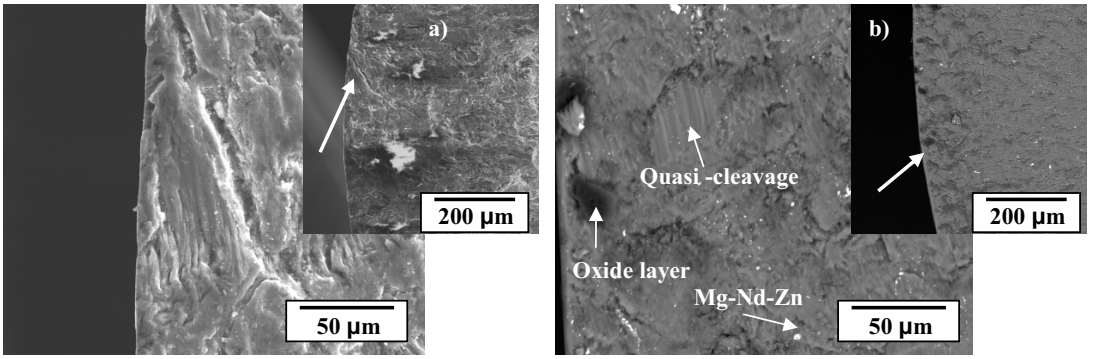

Fig. 5. SEM images (SE) of the fracture surface of the AZ31 alloy after fatigue testing (±120 MPa, 2.6 x10^5 cycles), SEM images (BSE) of the fracture surface of the ZN11 alloy after fatigue testing (±110 MPa, 2.1 x10^4 cycles). The white arrows indicate the crack initiation sites.

The crack front profiles of the AZ31 and ZN11 samples after fatigue testing are shown in Figs. 6 and 7, respectively. In the AZ31 alloy, micro-cracks are observed near the crack surface. These micro-cracks appear to be inter-granular and are located mainly along twin boundaries. Furthermore, a high density of twins is observed especially in the larger grains. With regard to the crack front profile in ZN11, micro-cracks are also found near to twin boundaries. However, most of the micro-cracks propagating in an inter-granular mode do not develop at twin boundaries.

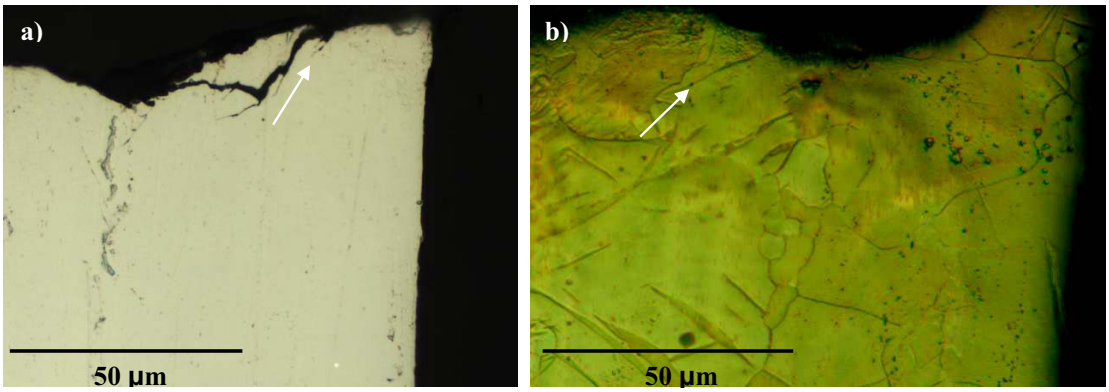

Fig. 6. Crack front profiles of the AZ31 alloy (±140 MPa, 9.1 x10^4 cycles), a) after mechanical polishing and b) after electrolytic polishing.The arrows indicate the micro-crack sites.

These results show that deformation produced by tensile twins could be the main factor in the crack initiation in the case of AZ31. As described previously, extensive {10-12} twinning occurs under compressive loading when

samples are tested parallel to the extrusion direction. Since twin boundaries can act as obstacles to dislocation glide [15], local stress concentrations are formed which lead to crack initiation. In AZ31, the endurance limit of 90 MPa at 10^7 cycles is lower than the compressive yield strength. It is important to note that the extruded AZ31 alloy has an inhomogeneous microstructure (Fig. 1b) and that the larger and unrecrystallised grains tend to show a high density of tensile twins.

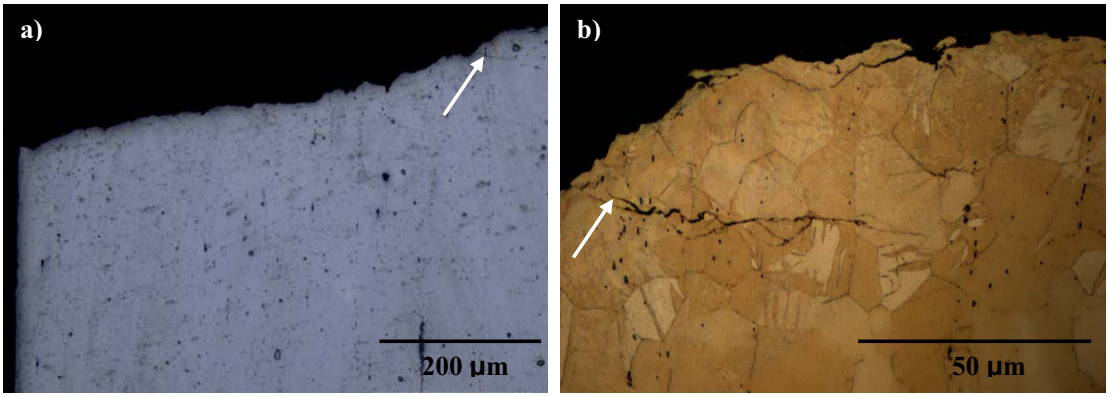

Fig. 7. Crack front profiles of the ZN11 alloy (±100 MPa, 3.2 x10^4 cycles), a) after mechanical polishing and b) after etching. The arrows indicate the micro-crack sites.

The fracture surfaces suggest that the crack initiation mechanism in ZN11 is mainly due to cyclic slip deformation. Fatigue failure is thought to result from the interactions between slip bands and Mg-Nd-Zn particles and grain boundaries which hinder the slip band activity and generate high, local stress concentrations. Deformation by twinning is not considered to be a significant factor for crack initiation in ZN11 due to its weak texture. A further possible factor contributing to the fatigue failure mechanism in the ZN11 alloy is the stress concentration created at the oxide layer, since the oxide layer could act as a barrier to the intrusions and extrusions caused by slip bands. Xu et al. [12] have also reported that the stress concentrations produced by the above mechanism could lead to crack formation in RE-containing Mg alloys.

4. Conclusions

The mechanical properties of AZ31 and ZN11 were investigated. Differences in the microstructure, texture and mechanical response were correlated with the micro-mechanisms of crack initiation. The AZ31 alloy was characterised by an inhomogeneous structure and strong crystallographic texture, which led to mechanical asymmetry. In this case, the main factor responsible for fatigue crack initiation was the deformation produced by twinning. This phenomenon is explained by the strong fibre texture, which led to extensive {10-12} twinning under compressive loading. The alloy ZN11 was characterised by a homogeneous microstructure with recrystallised grains and a weak texture. As a consequence of the texture and microstructure, no yield asymmetry was observed. With regard to the fatigue properties, cyclic slip deformation was the main factor responsible for fatigue failure. This is explained by the hindrance of slip band activity and the generation of local stress concentrations that lead to crack initiation.

Acknowledgements

The authors are grateful to Dr. Peter Beaven at GKSS Research Centre for fruitful discussions and to Dr.-Ing. Sören Müller for his technical assistance with the extrusion experiments at the Extrusion Research Centre at the University of Technology, Berlin, Germany.

References

[1] P. Zhang, J. Lindemann, Influence of shot peening on high cycle fatigue properties of the high-strength wrought magnesium alloy AZ80, *Scripta Mater.* **52** (2005), pp. 485-490.

[2] Z-H. Liu, E-H. Han, L. Liu., High-cycle fatigue behavior of Mg–Zn–Y–Zr alloy, *Mater. Sci. Eng.* **483-484** (2008), pp. 373-375.

[3] S. Hasegawa, Y. Tsuchida, H. Yano, M. Matsui, Evaluation of low cycle fatigue life in AZ31 magnesium alloy, *Int. J. Fatigue* **29** (2007), p. 1839.

[4] Q.Y. Wang, C. Bathias, N. Kawagoishi, Q. Chen, Effect of inclusion on subsurface crack initiation and gigacycle fatigue strength, *Int. J. Fatigue* **24** (2002), pp. 1269-1274.

[5] H. Mughrabi, On the life-controlling microstructural fatigue mechanisms in ductile metals and alloys in the gigacycle regime, *Fatigue Fract. Eng. Mater. Struct*. **22** (1999), pp. 633-641.

[6] H. Mughrabi, Specific features and mechanisms of fatigue in the ultrahigh-cycle regime, *Int. J. Fatigue* **28** (2006), pp. 1501-1508.

[7] D.K. Xu, L. Liu., Y.B. Xu, E.H. Han, The crack initiation mechanism of the forged Mg–Zn–Y–Zr alloy in the super-long fatigue life regime, *Scripta Mater.* **56** (2007), pp. 1-4.

[8] F. Yang, S.M. Yin, S.X. Li, Z.F. Zhang, Crack initiation mechanism of extruded AZ31 magnesium alloy in the very high cycle fatigue regime, *Mater. Sci. Eng. A* **491** (2008), pp. 131-136.

[9] N. Stanford, M.R. Barnett, Effect of microalloying with rare-earth elements on the texture of extruded magnesium-based alloys, *Mater. Sci. Eng. A* **496** (2008), pp. 399-408

[10] Y. Chino, K. Sassa, M. Mabuchi, Texture and stretch formability of a rolled Mg–Zn alloy containing dilute content of Y, *Mater. Sci. Eng. A* **513-514** (2009), pp. 394-400

[11] V. Kree, J. Bohlen, D. Letzig, K.U. Kainer, Metallographische Gefügeuntersuchungen von Magnesiumlegierungen, *Praktische Metallographie* (2004), pp. 233-246

[12] K. Hantzsche, J. Bohlen, J. Wendt, K.U. Kainer, S. Yi, D. Letzig, Effect of rare earth additions on microstructure and texture development of magnesium alloy sheets, *Scripta Mater*., doi10.1016/2009.12.033, in press

[13] J. Bohlen, S.B. Yi, J. Swiostek, D. Letzig, H.G. Brokmeier, K.U. Kainer, Microstructure and texture development during hydrostatic extrusion of magnesium alloy AZ31, *Scripta Mater*. **53** (2005), pp. 259-264

[14] D. Wenjiang, L. Daquan, W. Qudong, L. Quiang , Microstructure and mechanical properties of hot-rolled Mg–Zn–Nd–Zr alloys, *Mater. Sci. Eng. A*, **483-484** (2008), pp. 228-230

[15] L. Fuskova, S. Yi, L. Nascimento, J. Bohlen, D. Letizig, K.U. Kainer, Comparison of Quasi-static and Cyclic Plastic Behaviour of a Wrought Magnesium Alloy, *Proceedings of TMS*, San Francisco (2009), pp. 81-84.

[16] T. Laser , Ch. Hartig , M.R. Nu¨rnberg , D. Letzig, R. Bormann, The influence of calcium and cerium mischmetal on the microstructural evolution of Mg–3Al–1Zn during extrusion and resulting mechanical properties, *Acta Mater.* , **56** (2008), pp 2791-2798.

[17] M.R. Barnett, Z. Keshavarz, A.G. Beer, D. Atwell,Influence of grain size on the compressive deformation of wrought Mg–3Al–1Zn, *Acta Mater*., **52** (2004), pp. 5093-5103.

[18] J. Bohlen, P. Dobron, J. Swiostek, D. Letzig, F. Chmelík, P. Lukac, K.U. Kainer, On the influence of the grain size and solute content on the AE response of magnesium alloys tested in tension and compression, *Mater. Sci. Eng. A,* **462** (2007), pp. 302-306.